J. Fluid Mech. (1978), *vol.* 88, *part* 3, *pp.* 541–562
Printed in Great Britain

Models of the scalar spectrum for turbulent advection

By R. J. HILL

Wave Propagation Laboratory, Environmental Research Laboratories, National Oceanic and Atmospheric Administration, Boulder, Colorado 80302

(Received 9 August 1977 and in revised form 22 February 1978)

Several models are developed for the high-wavenumber portion of the spectral transfer function of scalar quantities advected by high-Reynolds-number, locally isotropic turbulent flow. These models are applicable for arbitrary Prandtl or Schmidt number, ν/D, and the resultant scalar spectra are compared with several experiments having different ν/D. The 'bump' in the temperature spectrum of air observed over land is shown to be due to a tendency toward a viscous–convective range and the presence of this bump is consistent with experiments for large ν/D. The wavenumbers defining the transition between the inertial–convective range and viscous–convective range for asymptotically large ν/D (denoted k^* and k_1^* for the three- and one-dimensional spectra) are determined by comparison of the models with experiments. A measurement of the transitional wavenumber k_1^* [denoted $(k_1^*)_{\text{meas}}$] is found to depend on ν/D and on any filter cut-off. On the basis of the k^* values it is shown that measurements of β_1 from temperature spectra in moderate Reynolds number turbulence in air ($\nu/D = 0{\cdot}72$) may be over-estimates and that the inertial–diffusive range of temperature fluctuations in mercury ($\nu/D \simeq 0{\cdot}02$) is of very limited extent.

1. Introduction

Knowledge of the spatial power spectra of temperature and humidity fluctuations in turbulent flow is needed in treating the propagation and scattering of sound, optical, and radio frequency waves. The importance of such scalar fluctuations lies in their influence on the refractive index fluctuations in turbulent media. Four models of the scalar spectrum are developed for arbitrary Prandtl or Schmidt numbers; these models are applicable to high Reynolds number flows. The models give a unified treatment of scalar spectra for arbitrary Prandtl or Schmidt numbers; therefore, fitting the models to existing data allows one to predict the shape of scalar spectra that have not been measured, an example being the humidity spectrum at wavenumbers higher than can be observed by present techniques. The models are presented in § 4 after reviewing the observational data and previous models of the scalar spectrum.

The three-dimensional scalar spectrum $\Gamma(k, t)$ and its one-dimensional counterpart $\Psi(k_1, t)$ are herein normalized so that they are the spectral budgets of the mean-squared scalar fluctuation:

$$\langle n^2 \rangle = \int_0^\infty \Gamma(k, t)\, dk = \int_0^\infty \Psi(k_1, t)\, dk_1,$$

where n is the fluctuation in the concentration or temperature. Assuming isotropy, the diffusive dissipation rate χ of the mean-squared fluctuations is then given by

$$\chi = 2D\int_0^\infty k^2\,\Gamma(k,t)\,dk = 6D\int_0^\infty k_1^2\,\Psi(k_1,t)\,dk_1, \tag{1}$$

where D is the diffusivity. The relationship between $\Gamma(k,t)$ and $\Psi(k_1,t)$ is given by

$$\Psi(k_1,t) = \int_{k_1}^\infty \frac{\Gamma(k,t)}{k}\,dk. \tag{2}$$

There are several possible wavenumber ranges for the scalar spectrum depending on the ratio ν/D (ν being the kinematic viscosity) which is the Prandtl number Pr for temperature, or the Schmidt number Sc for molecular species. The terminology for these wavenumber ranges depends first on whether the wavenumber lies in the inertial or viscous range of the energy spectrum and second on whether the wavenumber lies in the convective or diffusive range of the scalar spectrum. For $\nu \gg D$ there may exist an inertial–convective range, a viscous–convective range, and a viscous–diffusive range. For $\nu \ll D$ the important wavenumber ranges are the inertial–convective and inertial–diffusive ranges.

For the scalar field the set of similarity parameters is χ, ϵ, ν, D, and the wavenumber k (Gibson 1968), where ϵ is the rate of viscous dissipation of turbulent kinetic energy per unit mass of fluid. Three useful scaling wavenumbers may be constructed from this set of parameters:

$$k_d \equiv (\epsilon/\nu^3)^{\frac{1}{4}}, \quad k_b \equiv (\epsilon/\nu D^2)^{\frac{1}{4}}, \quad k_c \equiv (\epsilon/D^3)^{\frac{1}{4}};$$

these are the Kolmogorov, Batchelor, and Corrsin wavenumbers, respectively. It was Batchelor (1959) who clarified the fact that k_b and k_c parameterize the rapid decrease in the scalar spectrum due to diffusion for the cases $\nu \gg D$ and $\nu \ll D$, respectively. It is useful to denote by k_L a wavenumber that is characteristic of the wavenumbers at which the turbulence contains most of its energy and at which the scalar field contains most of its mean-squared fluctuation. The similarity parameters may be rearranged by forming two non-dimensional parameters, ν/D and k/k_d, to give the set $\chi, \epsilon, \nu, \nu/D$, and k/k_d. Dimensional analysis then gives (Boston & Burling 1972; Gibson 1968)

$$\Gamma(k) = \chi\epsilon^{-\frac{1}{4}}\nu^{\frac{1}{4}}\,H(\nu/D,\, k/k_d), \quad k \gg k_L, \tag{3}$$

where H is a non-dimensional function. The use of ν rather than D as a scaling parameter, or the use of k_d to scale the wavenumber rather than k_b or k_c, is arbitrary owing to the existence of the non-dimensional parameter ν/D.

The dimensional analysis for the inertial–convective range does not include the parameters ν or D as dissipation is not an important process for this range. The results of Oboukhov (1949) and Corrsin (1951) for the inertial–convective scalar spectrum show that

$$\Gamma(k) = \beta\chi\epsilon^{-\frac{1}{3}}k^{-\frac{5}{3}} \quad \text{for} \quad k_L \ll k \ll \text{smaller of } k_d \text{ and } k_c, \tag{4}$$

where β is a non-dimensional constant which we call the Oboukhov–Corrsin constant. The requirement that k be much smaller than either k_d or k_c merely limits the inertial–convective range to wavenumbers below those at which viscosity or diffusion is important.

A unified treatment of the viscous–convective and viscous–diffusive ranges is given

by Batchelor (1959). His theory assumes that, at viscous-range length scales, the velocity field has spatial variation that is smooth relative to the spatial variation of a scalar having $D \ll \nu$. Batchelor shows that the local gradients of the scalar become aligned with the local axis of the least principal rate of strain and that the local gradients increase because of the straining while the amplitude of the fluctuation is decreased by diffusion. The typical time for a change in magnitude of the local rate of strain or for a rotation of the local principal axes of the rate-of-strain tensor relative to the fluid is assumed to be long compared with the lifetime of a given scalar fluctuation. Thus the velocity field is considered as a temporally persistent and spatially uniform straining describable by a single effective least principal rate of strain γ. The deduction for the scalar spectrum in the viscous–convective and viscous–diffusive ranges is

$$\Gamma(k) = -\chi\gamma^{-1}k^{-1}\exp(Dk^2/\gamma) \quad \text{for} \quad k \geqslant k_d. \tag{5}$$

Batchelor estimates the parameter γ as $-0{\cdot}5(\epsilon/\nu)^{\frac{1}{2}}$ in which case the argument of the exponent in (5) is $-2(k/k_b)^2$. If $k \ll k_b$ then the exponential in (5) is nearly unity and the viscous–convective spectrum becomes

$$\Gamma(k) = -\chi\gamma^{-1}k^{-1} \quad \text{for} \quad k_d \leqslant k \ll k_b. \tag{6}$$

Equation (6) may be obtained by dimensional analysis with parameters χ, γ, and k.

Kraichnan (1968) has estimated the effect of allowing γ to have large but infrequent local deviations from its usual value. The result of such spatial fluctuations in γ is that the k^{-1} viscous–convective power law is unchanged but the viscous–diffusive range decreases more gently than the Gaussian decrease predicted by Batchelor. Kraichnan found that the viscous–diffusive range was dominated by the infrequent occurrences of the very large values of γ, but the viscous–convective range was dominated by the typical occurrence of the moderate values of γ.

For the inertial–diffusive range Batchelor, Howells & Townsend (1959) hypothesize that the dominant contributions to $\Gamma(k)$ at wavenumber k are due to motions of the fluid with a scale size of k^{-1} acting on gradients in the scalar concentration that are nearly spatially uniform owing to the action of diffusion. Since most of the diffusive dissipation of the scalar spectrum occurs in the lowest wavenumber region of the inertial–diffusive range, Batchelor *et al.* (1959) set these gradients equal to the root-mean-square gradient of the scalar fluctuations. Their prediction is given by:

$$\Gamma(k) = \tfrac{1}{3}\alpha\chi\epsilon^{\frac{3}{4}}D^{-3}k^{-\frac{17}{3}} \quad \text{for} \quad k_c \ll k \ll k_d, \tag{7}$$

where α is the Kolmogorov constant. An alternative theory for the inertial–diffusive range by Gibson (1968) gives $\Gamma(k) \propto k^{-3}$.

2. Observations of the scalar spectrum

The $k^{-\frac{5}{3}}$ power law in the inertial–convective range is observed in a number of experiments: sodium chloride and temperature fluctuations in water by Gibson & Schwarz (1963); temperature fluctuations in water by Grant *et al.* (1968); ammonium acetate solute in water by Gibson, Lyon & Hirshsohn (1970*a*); temperature fluctuations in the atmospheric boundary layer by Pond *et al.* (1966), Gibson, Stegen & Williams (1970*b*), Boston & Burling (1972), Williams & Paulson (1977), and Champagne *et al.* (1977).

The k^{-1} power law in the viscous–convective range is strikingly verified by Grant *et al.* (1968) from temperature fluctuations in the ocean and by Gibson *et al.* (1970*a*) from ammonium acetate fluctuations ($Sc \gg 1$). The k^{-1} behaviour is also observed in the temperature ($Pr \simeq 7$) and sodium chloride ($Sc \simeq 700$) fluctuations in water as measured by Gibson & Schwarz (1963), and in the measurements of dye fluctuations in water ($Sc \simeq 2 \times 10^4$) by Nye & Brodkey (1967) and by McKelvey *et al.* (1975). No inertial–convective range was expected or observed in these latter two experiments.

There are very few measurements of scalar spectra for which the Prandtl or Schmidt number is small compared with unity. Measurement of the temperature spectrum in mercury ($Pr \simeq 0{\cdot}02$) was undertaken by Clay (1973) and by Rust & Sesonske (1966). Experiments have been performed on turbulent flow in weakly ionized argon gas ($Sc \simeq 0{\cdot}07$) passing through a discharge tube (Granatstein, Levine & Subramanian 1971; Garosi, Bekefi & Schulz 1970; Kuyel & Gruber 1973). Unfortunately these flows are at low Reynolds numbers; there are strong fluctuations in the neutral-gas temperature, and the velocity and ionization distributions are strongly inhomogeneous with thrashing of the plasma column observed. Thus, interpretation of the experiments in terms of local similarity theory appears impossible. Nevertheless, Bugnolo (1972) uses a Heisenberg model to describe the ionization-concentration spectrum. The effects that Bugnolo (1972) identifies as inertial–diffusive behaviour are shown by Kuyel & Gruber (1973) to be due to strong fluctuations in the density of the neutral gas.

In conclusion, the $k^{-\frac{5}{3}}$ inertial–convective law and the k^{-1} viscous–convective law appear well supported. Moreover, the scaling expressed by (3) appears adequate in those cases in which it has been tested. Unfortunately the diffusive ranges have not been adequately resolved except in the case of temperature fluctuations in air ($Pr \simeq 0{\cdot}72$) and in mercury ($Pr \simeq 0{\cdot}02$).

The value of the Oboukhov–Corrsin constant β, which appears in (4), may be obtained from one-dimensional temperature spectra when an inertial–convective range is in evidence, and by indirect estimates, which are summarized by Paquin & Pond (1971). In an inertial–convective range the one-dimensional temperature spectrum has the same form as the three-dimensional temperature spectrum in (4) with β replaced by a different constant β_1; isotropy implies $\beta = \frac{5}{3}\beta_1$. The indirect estimates of β_1 reviewed by Paquin & Pond (1971) indicate a value of about 0·38. The values of β_1 determined from observation of an inertial–convective range are as follows: Gibson & Schwarz (1963), 0·35; Grant *et al.* (1968), $0{\cdot}31 \pm 0{\cdot}06$; Lin & Lin (1973), $0{\cdot}6 \pm 0{\cdot}06$; Williams & Paulson (1977) data, $0{\cdot}50 \pm 0{\cdot}02$; Champagne *et al.* (1977), 0·41; Boston & Burling (1972), $0{\cdot}76 \pm 0{\cdot}02$;† Gibson *et al.* (1970*b*), 1·16 and Clay (1973) obtained

$$\beta_1 = 0{\cdot}55 \pm 0{\cdot}05, \quad 0{\cdot}56 \pm 0{\cdot}02 \quad \text{and} \quad 0{\cdot}52 \pm 0{\cdot}13$$

from temperature spectra in water, air, and mercury. The data of Gibson *et al.* (1970*b*) and Boston & Burling (1972) were obtained in the boundary layer over the ocean and a tidal flat, respectively. Recently, it has been shown by Schmitt, Friehe & Gibson (1978) that contamination of the fluctuating temperature signal can occur by salt spray depositing on resistance wire sensors. The contaminated sensors then respond to humidity as well as temperature fluctuations. This contamination is present in the

† We obtain $\beta_1 = 0{\cdot}76$ by rescaling the Boston & Burling (1972) data so that the area under the scaled dissipation spectrum is $\frac{1}{3}Pr$ where $Pr = 0{\cdot}72$.

Gibson *et al.* (1970*b*) data (C. A. Friehe, private communication), and may therefore explain their large β_1 value (Schmitt *et al.* 1978).

The β_1 determinations by Boston & Burling (1972), Williams & Paulson (1977), and Champagne *et al.* (1977) used a scalar dissipation rate determined by integrating the dissipation spectrum. The temperature spectral shapes found by Williams & Paulson and by Champagne *et al.* are in good agreement with each other and show a 'bump' at high wavenumbers. This bump also appears in the high-Reynolds-number air-jet data obtained by McConnell (1976). Such a bump is not evident in the Boston & Burling data, and the reasons for the discrepancy between their measurements and those of Williams & Paulson and of Champagne *et al.* are not clear. If the data of Gibson *et al.* (1970*b*) and Boston & Burling (1972) are excluded because of the salt-spray contamination problem, then the bump in the temperature spectrum in air appears to be a consistently observed feature for high-Reynolds-number turbulence.

The existence of the bump implies that β_1 should be determined from spectral values at wavenumbers such that $k/k_d \lesssim 0{\cdot}03$. A determination of β_1 from temperature spectra in air obtained at moderate Reynolds numbers may have a substantial contribution from the bump if portions of the spectrum at $k/k_d > 0{\cdot}03$ are used; such a determination of β_1 is a misinterpretation of the data. Thus the β_1 value of $0{\cdot}6 \pm 0{\cdot}06$ determined from moderate Reynolds number turbulence by Lin & Lin (1973) is in better agreement with the β_1 values found by Champagne *et al.* (1977) and Williams & Paulson (1977) than is at first apparent. The existing data now seem sufficiently consistent that we should recommend that β_1 be considered to lie between 0·41 and 0·50, which is based mainly on the determinations by Champagne *et al.* (1977) and by Williams & Paulson (1977).

3. Previous models of scalar spectral transfer

The simplest case of an advected scalar is the conserved passive scalar that has the following continuity equation:

$$\frac{\partial N}{\partial t} + \mathbf{V}.\nabla N = D\nabla^2 N.$$

The equation for the scalar spectrum that follows from this continuity equation is

$$\frac{\partial \Gamma(k,t)}{\partial t} - T(k,t) = -2Dk^2\,\Gamma(k,t),$$

where $T(k,t)$ is the scalar spectral transfer function. The fact that one equation in two unknowns results is the closure problem due to the coupling of the continuity equation to the nonlinear Navier–Stokes equations. To avoid the closure problem a model for $T(k,t)$ is used.

In this section we consider models of the scalar spectral transfer function $T(k)$, in particular, those developed by Corrsin (1964), Pao (1964, 1965), Leith (1968), and Kraichnan (1968). It is useful to introduce the scalar spectral flux function $F(k)$, which is defined by

$$T(k) \equiv -\frac{\partial F(k)}{\partial k}.$$

Thus, in the steady-state case the scalar spectrum satisfies

$$\frac{\partial F(k)}{\partial k} = -2Dk^2\,\Gamma(k). \tag{8}$$

In the steady state $F(k) = \chi$ if k lies in a convective range.

Corrsin (1964, 1961) generalized an energy cascading concept, which was originated by Onsager (1949), to the case of turbulently advected scalars. The model consists of writing the spectral flux function in the form

$$F(k) = s(k)\,\Gamma(k). \tag{9}$$

Corrsin (1964) took $s(k)$ as $k/\tau(k)$, where $\tau(k)$ is a time scale obtained by dimensional analysis using the parameters k and $E(k)$; he then used Kolmogorov's inertial range form for $E(k)$. Corrsin (1964) has also shown that if $\tau(k) = -\gamma^{-1}$, where γ is an effective rate of strain, then one obtains (5) and (6) for the viscous–convective and viscous–diffusive ranges of Batchelor (1959).

Pao (1964, 1965) proposed that the scalar flux $F(k)$ is due to a continuous cascading in wavenumber space rather than as a geometrical progression as proposed by Onsager. Pao obtained $s(k)$ in the inertial–convective and inertial–diffusive ranges by dimensional analysis using the parameters ϵ and k, and in the viscous–convective and viscous–diffusive ranges using the parameters γ and k, where γ is an effective rate of strain. Pao (1964) showed that the dimensional result in the viscous range, namely $s(k) = -\gamma k$, is identical with the theory by Batchelor (1959). However, Pao (1965) has assumed that the inertial-range form of $s(k)$ is valid even for $k > k_d$ when $\nu \gg D$; this assumption contradicts the results of Batchelor (1959) for the viscous–convective and viscous–diffusive ranges, and is also inconsistent with the experimental evidence of Grant *et al.* (1968).

Using the Pao (1964) model for the flux function (8) becomes

$$\frac{\partial s(k)\,\Gamma(k)}{\partial k} = -2Dk^2\,\Gamma(k), \tag{10a}$$

where

$$s(k) = \beta^{-1}\epsilon^{\frac{1}{3}}k^{\frac{4}{3}} \quad \text{for} \quad k \ll k_d, \tag{10b}$$

$$s(k) = l\gamma k \quad \text{for} \quad k \gg k_d, \tag{10c}$$

and l is a non-dimensional negative constant.

The solutions to (10a) are

$$\Gamma(k) = \chi\beta\epsilon^{-\frac{1}{3}}k^{-\frac{4}{3}}\exp\left[-(3\beta/2)\,(k/k_c)^{\frac{4}{3}}\right], \quad k \ll k_d, \tag{11}$$

and

$$\Gamma(k) \propto k^{-1}\exp\left[-(D/l\gamma)\,k^2\right], \quad k \gg k_d, \tag{12}$$

where (4) is the boundary condition used to determine the proportionality constant in (11). In the inertial–convective range $k \ll k_c$ and (11) gives the $k^{-\frac{5}{3}}$ power law. For $D \gg \nu$ the exponential in (11) causes the scalar spectrum to decrease rapidly for $k > k_c$. Thus the decrease of the scalar spectrum in the inertial–diffusive range is given as an exponential of the four-thirds power of the wavenumber, which is more rapidly decreasing than the $k^{-1\frac{2}{3}}$ variation predicted by Batchelor *et al.* (1959) for the inertial–diffusive range. For $D \ll \nu$ it follows that $k_c \gg k_d$, and therefore the exponential in (11) is close to unity over the entire inertial–convective range. With $l = -1$ (12) is

identical with Batchelor's theory as expressed in (5). Unfortunately there is no connexion between the inertial-range and viscous-range forms for $s(k)$ in the Corrsin–Pao model.

A model called the diffusion approximation has been developed by Leith (1968) for a scalar field advected by turbulence. This model consists of a spectral flux function of the form

$$F = -D_s \frac{\partial Q_s}{\partial k}. \tag{13}$$

The product $D_s Q_s$ is obtained by dimensional analysis with the parameters $\Gamma(k)$, $E(k)$ and k.

Leith invokes the equilibrium solution of Lee (1952) in order to obtain D_s and Q_s from their product. The Lee equilibrium solution applies to non-dissipative systems that have a truncation in wave vector space so that there is a maximum wavenumber allowed. With no dissipation and no spectral transfer beyond the maximum wavenumber, the spectrum increases as k^2 in order that the spectral transfer from lower to higher wavenumbers shall be balanced by transfer from high to low wavenumbers. The relevance of truncating wave vector space in the absence of dissipation is obscure. Thus the relevance of the requirement that $\Gamma(k)$ should be proportional to k^2 in the absence of diffusive dissipation in unclear. With the assertion that $\Gamma(k) \propto k^2$ if $D = 0$, the analysis by Leith yields

$$D_s \propto k^{\frac{11}{3}} E(k)^{\frac{1}{2}},$$

$$Q_s = k^{-2}\,\Gamma(k).$$

In the inertial range Leith adopts the inertial-range form of the energy spectrum. The resulting steady-state solutions for the diffusion approximation are found by Leith to be modified Bessel functions. These solutions behave as $k^{-\frac{5}{3}}$ in the inertial–convective range and decrease more slowly in the inertial–diffusive range than does the Corrsin–Pao model. However, for sufficiently large k in the inertial–diffusive range the solutions of the diffusion approximation decrease faster than any negative power of the wavenumber. In particular the solutions of the diffusion approximation decrease faster, at sufficiently large k, than the $k^{-\frac{17}{3}}$ variation predicted by Batchelor *et al.* (1959).

Unfortunately, the diffusion approximation does not represent $\Gamma(k)$ well in the viscous ranges. It may be shown that the diffusion approximation is inconsistent with a power law variation of $\Gamma(k)$ if $E(k)$ is decreasing faster than a power of k. For increasing k, the decrease in $E(k)$ in the viscous range causes a decrease in the diffusion approximation for scalar flux $F(k)$; consequently $\Gamma(k)$, as predicted by the diffusion approximation, increases markedly in the viscous–convective range for large Pr or Sc. It is concluded that the usefulness of the diffusion approximation is restricted to Pr or Sc less than unity.

A model of the scalar spectral transfer function for the viscous–convective and viscous–diffusive ranges of a scalar satisfying Pr or $Sc \gg 1$ is given by Kraichnan (1968). The spectral flux function for Kraichnan's model is given by

$$F(k) = \frac{\Lambda}{15} k^4 \frac{\partial}{\partial k}[k^{-2}\,\Gamma(k)], \tag{14}$$

where Λ is independent of wavenumber.

For Kraichnan's model the solution in the steady state is given by Mjolsness (1975) as

$$\Gamma(k) = 5(\chi/\Lambda)\, k^{-1}(1+\rho)\exp(-\rho), \tag{15}$$

where $$\rho \equiv (30D/\Lambda)^{\frac{1}{2}}\, k.$$

If $\rho \ll 1$, then (15) gives $\Gamma(k) \propto k^{-1}$, which is the viscous–convective dependence predicted by Batchelor (1959). In the viscous–diffusive range we have $\rho \gg 1$ and (15) gives $\Gamma(k) \propto \exp(-\rho)$; this exponential decrease of the scalar spectrum in the viscous–diffusive range is much more gradual than that in (5).

4. Models of the scalar spectrum for arbitrary ν/D

In this section we describe four models of the scalar spectral transfer function $F(k)$. We seek simple models that are capable of quantitatively describing the entire high-wavenumber portion of the scalar spectrum for arbitrary ν/D. Recognizing that such models are basically speculative, we desire to keep the models as simple as possible. In particular, the scalar spectral transfer function $T(k)$ shall not contain the energy spectrum $E(k)$ because the shape of the energy spectrum is not known in detail in the viscous range. Furthermore, we require that the models have empirical support; that is, their predictions must adequately agree with available experiments. All of the models described have the $k^{-\frac{5}{3}}$ inertial–convective and k^{-1} viscous–convective behaviours; the models differ mainly in their predictions for the diffusive ranges and for the transition between the inertial–convective and viscous–convective ranges. These models are generalizations of the Corrsin–Pao model and of the models of Leith and Kraichnan, which are reviewed in the previous section.

For large Prandtl or Schmidt number the scalar spectrum makes a transition from a $-\frac{5}{3}$ power law in the inertial–convective range to a -1 power law in the viscous–convective range; the average of these exponents is $-\frac{4}{3}$. We locate the transition between these two ranges by the transitional wavenumber k^*. Specifically, we define k^* as the wavenumber between the inertial–convective and viscous–convective ranges at which

$$\left.\frac{\partial \ln \Gamma(k)}{\partial \ln k}\right|_{k=k^*} = -\tfrac{4}{3} \quad \text{for} \quad D \ll \nu. \tag{16}$$

Although k^* is defined in (16) only for $D \ll \nu$, the models that follow give k^* significance even for $D \gg \nu$. In the model spectra for $D \gg \nu$, k^* is a wavenumber at which a transition occurs between an inertial–diffusive range at wavenumbers lower than k^* and a viscous–diffusive range at higher wavenumbers. The one-dimensional scalar spectrum $\Psi(k_1)$ also makes a transition between the inertial–convective and viscous–convective range for $D \ll \nu$; we define this second transitional wavenumber k_1^* by

$$\left.\frac{\partial \ln \Psi(k_1)}{\partial \ln k_1}\right|_{k_1=k_1^*} = -\tfrac{4}{3} \quad \text{for} \quad D \ll \nu. \tag{17}$$

We anticipate that k^* and k_1^* are not equal and that $k_1^* < k^*$. If a simple model having $\Gamma(k) \propto k^{-\frac{5}{3}}$ for $k < k^*$ and $\Gamma(k) \propto k^{-1}$ for $k > k^*$ is substituted into (2) and (17) then k^* is found to be roughly twice as large as k_1^*. The ratio k^*/k_1^* is found on the basis of a model in § 5.3. Moreover, if k^*/k_d is a constant then k_1^*/k_d is expected to be a function of ν/D.

The results of the following analysis are expressed using Kolmogorov scaling for $\Gamma(k)$ and $\Psi(k)$, that is, the following non-dimensional scalar spectra are used:

$$\tilde{\Gamma}(k) \equiv \frac{k_d^3 \nu}{\chi} \Gamma(k).$$

$$\tilde{\Psi}(k) \equiv \frac{k_d^3 \nu}{\chi} \Psi(k).$$

4.1. *Model* 1

The first model is an extension to the case of scalar advection of the model for energy transfer developed by Lin (1972). Two time scales are defined as follows:

$$\tau_1 = \epsilon^{-\frac{1}{3}} k^{-\frac{2}{3}}, \quad \tau_2 = Q(\nu/\epsilon)^{\frac{1}{2}}. \tag{18}$$

The time scale τ_1 exceeds τ_2 in the inertial range whereas the opposite is true in the viscous range. The non-dimensional constant Q is a free parameter to be determined by comparison with experiment.

The Corrsin–Pao model is used by taking the function $s(k)$ in (9) to be

$$s(k) = \frac{\beta^{-1} k}{\tau_1 + \tau_2}.$$

This form satisfies the requirement that $s(k)\,\Gamma(k) \to \chi$ in the inertial–convective range when (4) is used for $\Gamma(k)$. A non-dimensional wavenumber y is defined as $y \equiv Q^{\frac{3}{4}} k/k_d$. From (10*a*) the equation for the scalar spectrum is

$$A^{-1} \frac{d}{dy}\left[\frac{y^{\frac{5}{3}}\,\Gamma(y)}{1+y^{\frac{2}{3}}}\right] = -2y^2\Gamma(y),$$

where $A \equiv \beta Q^{-2} Pr^{-1}$.

This equation is solved subject to (1) and yields the following Kolmogorov-scaled spectrum:

$$\tilde{\Gamma}(y) = \beta Q^{\frac{5}{4}} y^{-\frac{5}{3}} (1+y^{\frac{2}{3}}) \exp\left[-A(\tfrac{3}{2} y^{\frac{4}{3}} + y^3)\right].$$

In the inertial–convective range this solution reduces to (4). In the limit $A \ll 1$ and $y \gg 1$ the solution reduces to (5) which is the viscous–convective and viscous–diffusive form predicted by Batchelor (1959) with the least principal rate-of-strain parameter given by $\gamma = -(Q\beta)^{-1}(\epsilon/\nu)^{\frac{1}{2}}$. The inertial–diffusive range is characterized by $Ay^{\frac{4}{3}} \gg 1$ and $y \ll 1$ in which case the above solution reduces to (11), which is the prediction of the Corrsin–Pao model for the inertial–diffusive range.

4.2. *Model* 2

This model is an extension of the Corrsin–Pao model in which it is required that $s(k)$ and $d \ln s(k)/d \ln k$ make a smooth transition between their inertial–convective and viscous–convective forms. The transition is located at the transitional wavenumber k^*, as defined in (16). The hyperbolic tangent is used to give the smooth transition in the above derivative of $s(k)$ and a parameter a is introduced which governs the width of the transition. It is assumed that

$$\frac{d \ln s(k)}{dz^*} = \tfrac{5}{3} - \tfrac{1}{3}[1 + \tanh(az^*)],$$

where $z^* \equiv \ln(k/k^*)$. Integrating this equation and requiring that $s(k)\,\Gamma(k) = \chi$ in the inertial–convective range yields

$$s(k) = \beta^{-1}\epsilon^{\frac{1}{3}}k^{\frac{5}{3}}[(k/k^*)^{2a} + 1]^{-1/(3a)}.$$

This $s(k)$ has the form of (10b, c) for $k \ll k^*$ and $k \gg k^*$, respectively. Model 1 is just a special case of this model with $a = \frac{1}{3}$.

The scalar spectrum is the solution of (10a) using the above $s(k)$. The solution is given in terms of the Kolmogorov-scaled spectrum $\tilde{\Gamma}$ as

$$\ln[\beta^{-1}(k^*/k_d)^{\frac{4}{3}}\tilde{\Gamma}(k)] = -\tfrac{4}{3}z^* + \frac{1}{3a}\ln[2\cosh(az^*)] - 2\beta(k^*/k_d)^{\frac{4}{3}}Pr^{-1}\int_{-\infty}^{z^*}\exp(5w/3)\,[2\cosh(aw)]^{1/(3a)}\,dw. \quad (19)$$

The above scalar spectrum has two free parameters to be determined by comparison with experiment: k^*/k_d locates the transition between inertial–convective and viscous–convective ranges, and a determines the width of the transition. This model will be successful in predicting scalar spectra for arbitrary ν/D only if the same values of (k^*/k_d) and a apply for all ν/D. For $z^* \lesssim -1$ the integral above may be approximated by $\frac{3}{4}\exp(\frac{4}{3}z^*)$. The appearance of the Prandtl number in the last term shows that this term describes the decrease of the spectrum in the diffusive ranges. For $k \ll k^*$, (19) reduces to (11), the exponential in (11) being significant only for $D \gg \nu$. Thus (19) yields the inertial–convective and inertial–diffusive predictions of the Corrsin–Pao model. For $k \gg k^*$, (19) becomes proportional to the spectrum in (5); for $D \ll \nu$ the proportionality becomes an equality with

$$\gamma = -\beta^{-1}(k^*/k_d)^{\frac{8}{3}}(\epsilon/\nu)^{\frac{1}{2}}.$$

Thus the viscous–convective and viscous–diffusive ranges predicted by Batchelor (1959) result from this model.

4.3. *Model* 3

The third model is different from the first two in that it is a diffusion model based on a spectral flux function having the form of (13) with $Q_s(k) = k^{-2}\,\Gamma(k)$. This model derives from the inertial-range form of Leith's diffusion approximation and from the viscous-range form of Kraichnan's flux function. The procedure introduced by Lin (1972) is now used to assert that the form of $D_s(k)$ at all high wavenumbers is obtained by dimensional analysis using the wavenumber and $(\tau_1 + \tau_2)$ from (18). The parametric wavenumber $k^s = k_d Q^{-\frac{3}{2}}$ is introduced and the flux function in (13) is required to satisfy $F(k) = \chi$ for wavenumbers in the inertial–convective range; the resulting $D_s(k)$ is

$$D_s(k) = \tfrac{3}{11}\beta^{-1}\epsilon^{\frac{1}{3}}\frac{k^{\frac{14}{3}}}{1 + (k/k^s)^{\frac{8}{3}}}.$$

The wavenumber k^s should not be confused with the transitional wavenumber k^* which is defined by (16). In terms of the non-dimensional wavenumber $y = k/k^s$ the equation for the scalar spectrum is

$$\frac{d}{dy}\left\{\frac{y^{\frac{14}{3}}}{1+y^{\frac{8}{3}}}\frac{d}{dy}[y^{-2}\,\Gamma(y)]\right\} = \tfrac{22}{3}\beta\,Pr^{-1}(k^s/k_d)^{\frac{4}{3}}\,y^2\,\Gamma(y).$$

This equation has one free parameter, namely k^s/k_d, which is to be chosen by comparison with experiment.

For $k \ll k^s$, $D_s(k) \propto \epsilon^{\frac{1}{3}} k^{-\frac{14}{3}}$, which is the inertial-range form of $D_s(k)$ given by Leith (1968), and this model gives (4) for the inertial–convective range; if, in addition, $D \gg \nu$ then the inertial–diffusive range form for $\Gamma(k)$ given by Leith (1968) results. For $k \gg k^s$, $D_s(k) \propto Q^{-1}(\epsilon/\nu)^{\frac{1}{2}} k^4$, which is similar to Kraichnan's (1968) model, and the solutions of this model are proportional to the scalar spectrum in (15) with the non-dimensional wavenumber $\rho = (22\beta/3)^{\frac{1}{2}} (k^s/k_d)^{-\frac{1}{3}} (k/k_b)$; if, in addition, $D \ll \nu$ then the proportionality becomes an equality with

$$\Lambda = (\tfrac{45}{11}) \beta^{-1} (\epsilon/\nu)^{\frac{1}{2}} (k^s/k_d)^{\frac{2}{3}}. \tag{20}$$

4.4. *Model* 4

The final model is also a diffusion model. In analogy with the second model, it is required that $D_s(k)$ and $d \ln D_s(k)/d \ln k$ make smooth transitions between their inertial-range and viscous-range formulae. As in the second model, the hyperbolic tangent is used to give the smooth transition to the above derivative of $D_s(k)$. Two parameters are introduced: the wavenumber $k^\dagger$ and a non-dimensional constant b which governs the width of the transition. The wavenumber $k^\dagger$ should not be confused with the transitional wavenumber k^* as defined by (16). It is assumed that

$$\frac{d \ln D_s}{dz^\dagger} = \tfrac{14}{3} - \tfrac{1}{3}[1 + \tanh(bz^\dagger)],$$

with $z^\dagger \equiv \ln(k/k^\dagger)$. Subject to the condition $F(k) = \chi$ in the inertial–convective range, we have

$$D_s(k) = \tfrac{3}{11} \beta^{-1} \epsilon^{\frac{1}{3}} k^{-\frac{14}{3}} [(k/k^\dagger)^{2b} + 1]^{-1/(3b)}.$$

In terms of the non-dimensional wavenumber $x \equiv k/k^\dagger$ the equation for the scalar spectrum is

$$\frac{d}{dx}\left\{x^{\frac{14}{3}} (x^{2b} + 1)^{-1/(3b)} \frac{d}{dx}[x^{-2}\Gamma(x)]\right\} = \tfrac{22}{3} \beta Pr^{-1} (k^\dagger/k_d)^{\frac{4}{3}} x^2 \Gamma(x).$$

This equation contains two free parameters to be determined by comparison with experiment, namely $(k^\dagger/k_d)$ and b. The asymptotic solutions of this equation are the same as those of model 3 with k^s replaced by $k^\dagger$. Model 3 is a special case of model 4 with $b = \frac{1}{3}$.

5. Comparison of the models with experiment

All four of the models described in the previous section yield scalar spectra with the $k^{-\frac{5}{3}}$ inertial–convective range form and the k^{-1} power law for the viscous–convective range. The differences between the models are illustrated in figure 1 for several Prandtl numbers; the values of the model parameters used for figure 1 are those obtained in the following by comparison with the data of Champagne *et al.* (1977).

All four model spectra are the solutions of linear, homogeneous differential equations; any such solution multiplied by a constant is also a solution. Therefore, the models are not capable of predicting a value of β, and β is used as an adjustable parameter when fitting data.

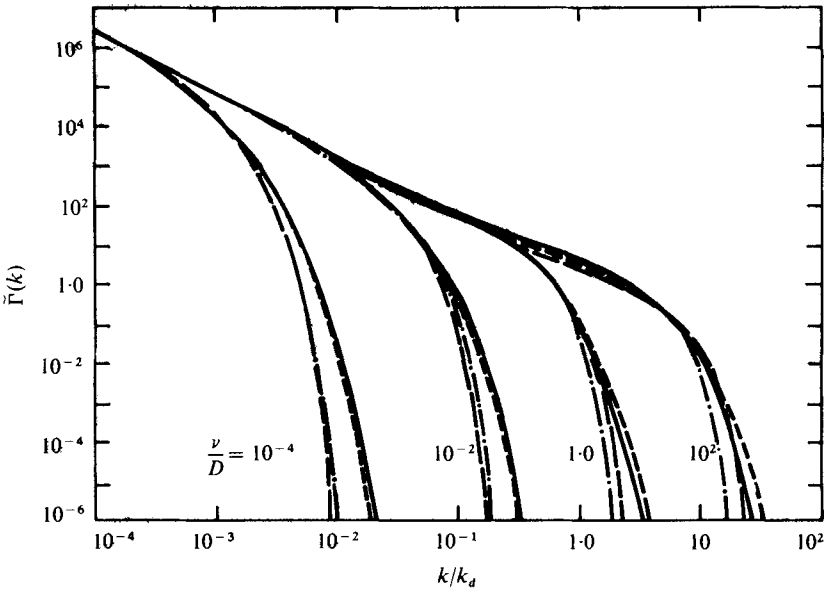

FIGURE 1. The model spectra for four values of ν/D. ---, model 1; —·—, model 2; · · · ·, model 3; ——, model 4.

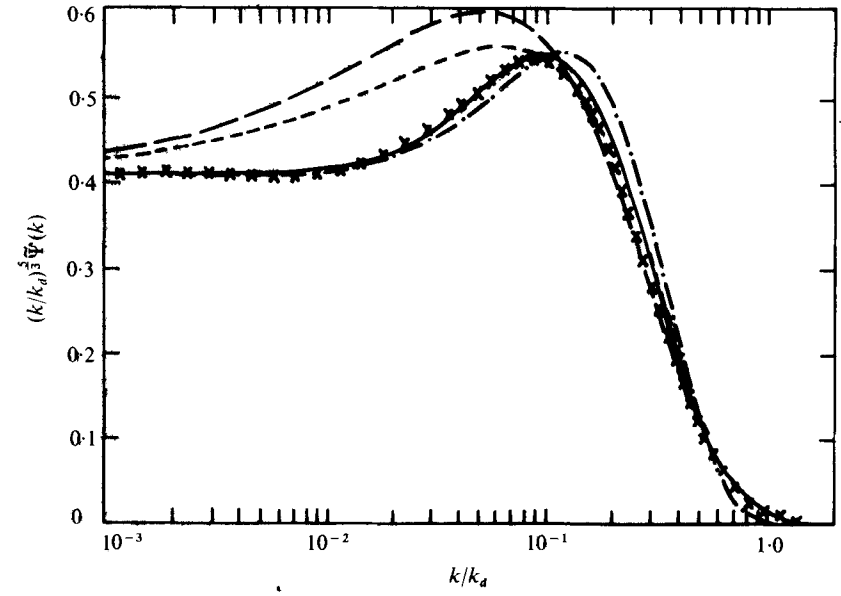

FIGURE 2. Comparison of the models with the data obtained by Champagne *et al.* (1977). ×, data. The symbols for the models are the same as in figure 1.

5.1. *Temperature fluctuations in the atmospheric surface layer*

We now compare the models with temperature spectra measured in the atmospheric surface layer by Champagne *et al.* (1977) and by Williams & Paulson (1977). No noise correction was found necessary by Champagne *et al.*, but a noise correction was used by Williams & Paulson. Both data sets were corrected for the aliasing due to the fluctuating

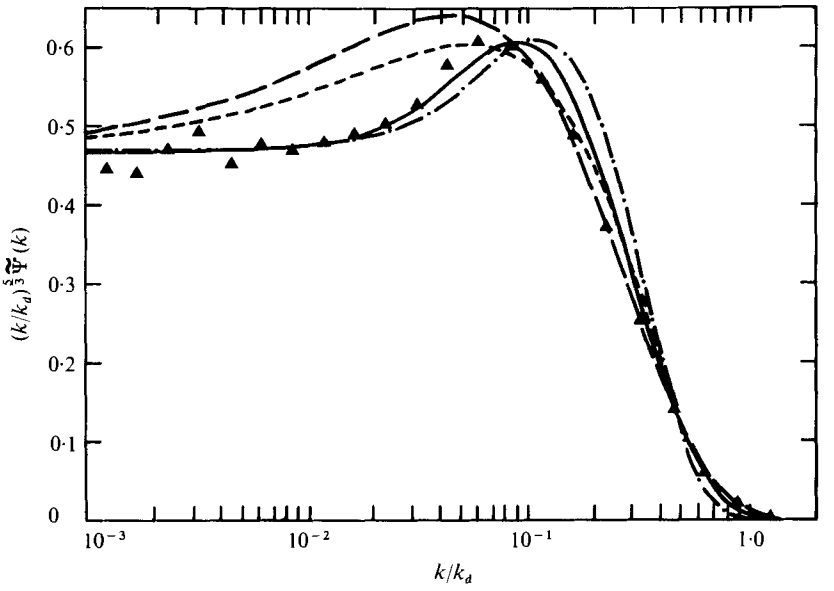

FIGURE 3. Comparison of the models with the data obtained by Williams & Paulson (1977). ▲, data. The symbols for the models are the same as in figure 1.

Data set	Model 1 Q	Model 2 k^*/k_d, a	Model 3 $k^\S/k_d$	Model 4 $k^\dagger/k_d$, b
Champagne *et al.*	2·5	0·074, 1·4	0·174	0·072, 1·9
Williams & Paulson	2·2	0·073, 1·7	0·22	0·071, 2·0

TABLE 1. Values of the model parameters.

convection velocity (Wyngaard & Clifford 1977). The one-dimensional spectra are computed for the models and are compared with the data in figures 2–7. The Prandtl number is taken to be 0·72, and the β_1 values used are 0·41 and 0·46 for the Champagne *et al.* data and Williams & Paulson 9-run-average, respectively. The values of the model parameters used for the figures are given in table 1.

Figures 2 and 3 present the function $(k/k_d)^{\frac{5}{3}}\tilde{\Psi}(k)$; this function is the constant β_1 in the inertial–convective range. Both data sets show a pronounced 'bump' at high wavenumbers; this bump is reflected in all four of the models. The 'bump' is the appearance of a tendency toward a viscous–convective range at wavenumbers lower than those at which diffusive dissipation sharply reduces the spectrum It is evident from figures 2 and 3 that models 1 and 3 have a much too gradual transition between the inertial–convective and viscous–convective ranges. In fact, the curves for models 1 and 3 closely approach the constant β_1 only for wavenumbers smaller than those shown in the figures. Consequently the parameters for these two models are chosen by matching the peak values of the model's dissipation spectra with those of the data. Models 2 and 4, on the other hand, reproduce the bump in the data quite well. The parameters for models 2 and 4 are then chosen to obtain a bump with about the same height and width as the data, without regard to the position of the bump maximum.

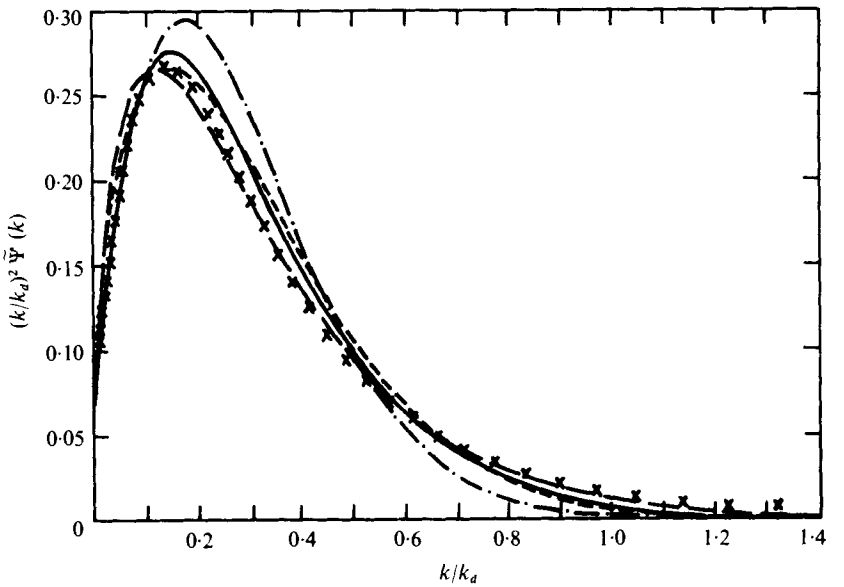

FIGURE 4. Comparison of the model one-dimensional dissipation spectra with the data obtained by Champagne *et al.* (1977). ×, data. The symbols for the models are the same as in figure 1.

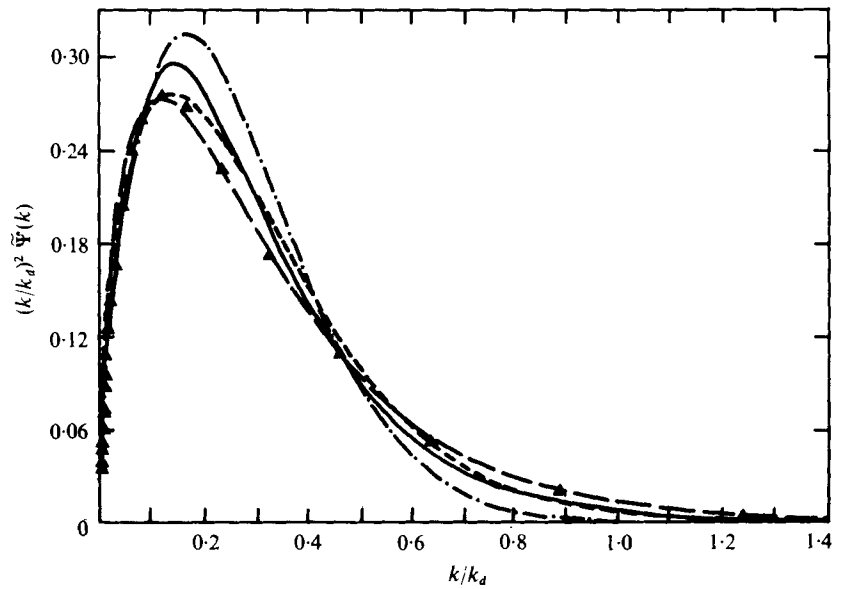

FIGURE 5. Comparison of the model one-dimensional dissipation spectra with the data obtained by Williams & Paulson (1977). ▲, data. The symbols for the models are the same as in figure 1.

The crosses (×) in figures 2, 4 and 6 are the result of applying the fluctuating-convection-velocity correction to a polynomial fit to the uncorrected data; the calculations were done by the experimenters. This polynomial fit is excellent for the dissipation spectrum and for the function $k^4\Psi(k)$. However, this polynomial fit slightly underestimates the height of the bump. It is seen in figure 2 that models 2 and 4 have a

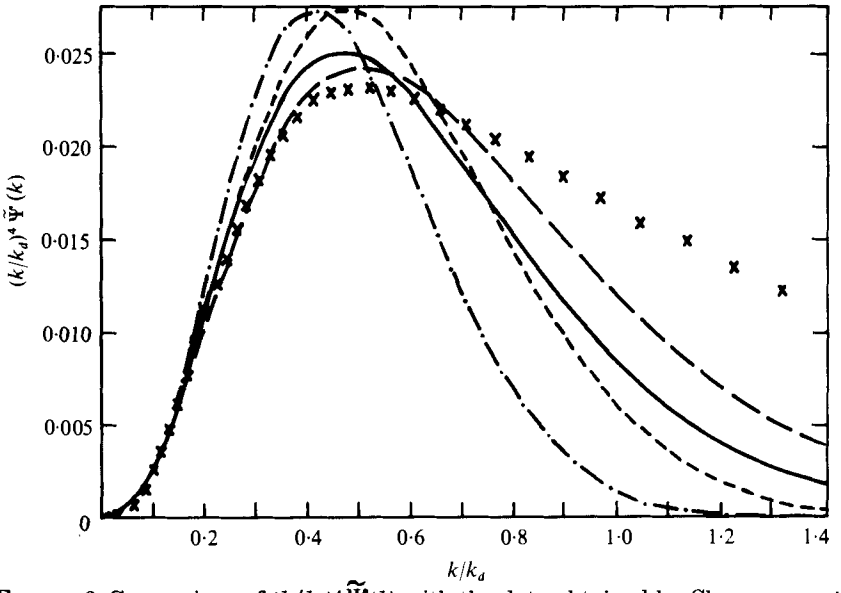

FIGURE 6. Comparison of $(k/k_d)^4\,\tilde{\Psi}(k)$ with the data obtained by Champagne *et al.* (1977). ×, data. The symbols for the models are the same as in figure 1.

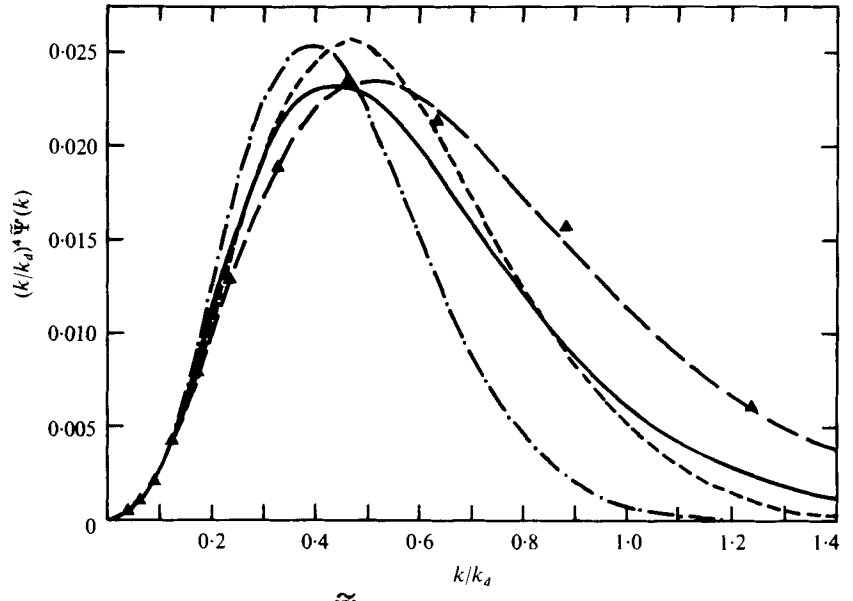

FIGURE 7. Comparison of $(k/k_d)^4\,\tilde{\Psi}(k)$ with the data obtained by Williams & Paulson (1977). ▲, data. The symbols for the models are the same as in figure 1.

slightly higher bump than the data; this is intentional in order to compensate for the bias in the polynomial fit to the data.

The scaled dissipation spectra are compared with the data in figures 4 and 5. By (1), the area under all of the curves must be the same, namely $\frac{1}{6}Pr$. A dissipation spectrum that falls more rapidly at high wavenumbers must then have a higher peak value at the

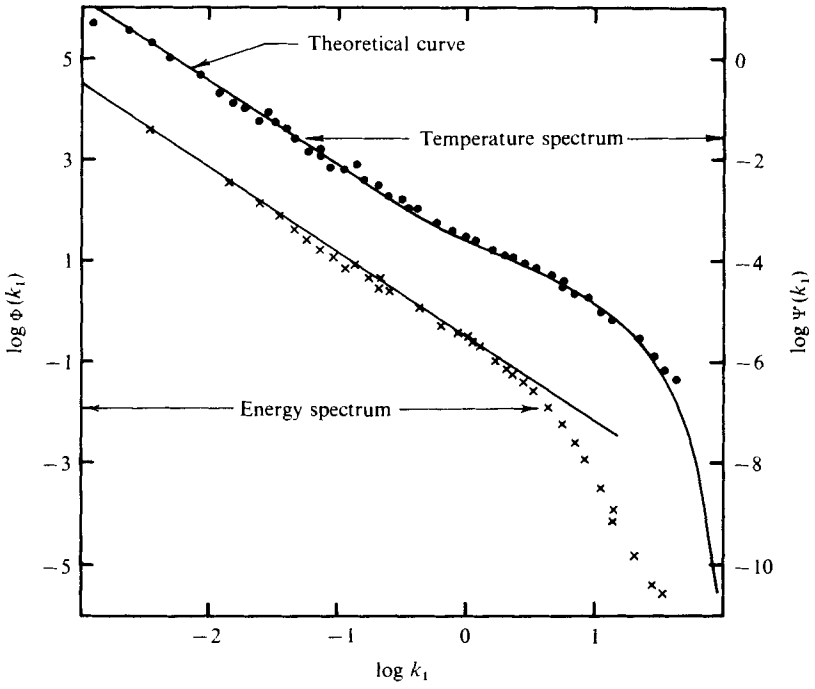

FIGURE 8. Comparison of model 2 with the one-dimensional temperature spectrum for run 2 of Grant *et al.* (1968). Also shown is the one-dimensional energy spectrum for their run 2.

lower wavenumbers. Comparing the position of the peak in the dissipation spectrum with the position of the bump maximum in figures 2 and 3 shows that a higher peak in the dissipation spectrum tends to move the bump maximum to higher wavenumbers. Model 2 has a relatively rapidly falling tail in the dissipation spectrum and consequently a higher peak in the dissipation spectrum; therefore the bump maximum is at a slightly higher wavenumber than the data. The above remarks are the motivation for ignoring the position of the bump maximum in fitting models 2 and 4 to the data.

Figures 6 and 7 present the fourth wavenumber moment of the scaled one-dimensional spectrum. In interpreting these figures, and also figures 4 and 5, it should be kept in mind that the accuracy of the data is questionable at $(k/k_d) \gtrsim 0{\cdot}8$. For instance, in figure 6 there is noise evident in the data for $k/k_d \gtrsim 0{\cdot}8$; the signal-to-noise ratio was unity at $k/k_d \simeq 1{\cdot}0$ (Champagne *et al.* 1977). If one could remove this noise then the data points would be lower at the higher wavenumbers, in better agreement with the model spectra. In figure 4 the area under the data and model curves must be $\frac{1}{6}Pr$, with $Pr = 0{\cdot}72$. If the tail of the data in figure 4 were reduced by a noise subtraction then the values near the peak would be increased, resulting in even better agreement with model 4.

5.2. *Temperature fluctuations in the ocean*

We compare the spectrum from model 2 with the one-dimensional temperature spectrum from the sea water measurements by Grant *et al.* (1968). The comparison with their run 2 is presented in figure 8 along with their one-dimensional energy spectrum

for that run. The thermal diffusivity used is the same as used by Grant *et al.* (1968), namely $1{\cdot}44 \times 10^{-3}\,\mathrm{cm^2\,s^{-1}}$. As is appropriate to the water temperature of their run 2 we take $Pr = 9{\cdot}2$. The value of k^*/k_d is taken to be 0·044. We use $\beta_1 = 0{\cdot}31$ as given by Grant *et al.* (1968) for their run 2. The values of β_1, k^*/k_d, and Pr are sufficient to determine $\tilde{\Gamma}(k)$. For run 2 Grant *et al.* (1968) give

$$\epsilon = 0{\cdot}52\,\mathrm{cm^2\,s^{-3}} \quad \text{and} \quad \chi = 4{\cdot}2 \times 10^{-3}\,^{\circ}\mathrm{K^2\,s^{-1}};$$

this is then sufficient information to determine the unscaled spectrum $\Psi(k_1)$, which is presented in figure 8. Owing to difficulties in comparing with data in graphical form, only model 2 is presented; however, comparison with figure 1 illustrates the differences between the models in the viscous–convective and viscous–diffusive ranges. However, model 4 and $Pr = 9{\cdot}2$ was used to obtain k^*/k_d based on the estimate by Grant *et al.* (1968) that $k_1^*/k_d = 0{\cdot}024 \pm 0{\cdot}008$; this resulted in $k^*/k_d = 0{\cdot}041 \pm 0{\cdot}013$, in good agreement with $k^*/k_d = 0{\cdot}044$ used in model 2 to produce figure 8.

In a stratified medium, such as the ocean, it is possible that 'fossil turbulence' contributes to measured temperature spectra. Grant *et al.* (1968) present temperature and energy spectra measured in both Discovery Passage and the open ocean. Their energy spectra from the open ocean have anomalous shapes with little or no inertial range, and it can be speculated that the corresponding temperature spectra may be contaminated by fossil turbulence. Their energy spectra from Discovery Passage, run 2 being an example, have two to three decades of inertial range, which implies active, high-Reynolds-number turbulence. Thus it is assumed that the temperature spectra from Discovery Passage are not affected by fossil turbulence.

5.3. *Comparison with ammonium acetate fluctuations*

Gibson *et al.* (1970*a*) have measured the spectrum of ammonium acetate fluctuations in a sphere wake at downstream positions of 2·17 and 7·5 diameters, which we refer to as runs 1 and 2 respectively. The data were low-pass filtered; the resultant filtered one-dimensional spectra have a transition from an inertial–convective to a viscous–convective range at the wavenumbers $0{\cdot}04k_d$ and $0{\cdot}03k_d$ for runs 1 and 2 respectively. We denote the measured transitional wavenumber by $(k_1^*)_{\mathrm{meas}}$ and investigate the relationship between $(k_1^*)_{\mathrm{meas}}$ and the transitional wavenumbers k_1^* and k^* as defined in (16) and (17). For this purpose, model 4 is used with $b = 1{\cdot}9$ and a Schmidt number of 700, although the results are insensitive to variation of the Schmidt number. In order to simulate the low-pass filter we truncate the integration in (2) at an upper limit of $0{\cdot}8k_d$ and $2{\cdot}0k_d$ (corresponding to experimental conditions) for runs 1 and 2 respectively; the resulting theoretical, filtered, one-dimensional spectra represent the data well and have the transition from inertial–convective to viscous–convective range at $0{\cdot}04k_d$ and $0{\cdot}03k_d$ if $k^\dagger/k_d$ is taken to be 0·09 and 0·075 for runs 1 and 2 respectively. The transitional wavenumber k_1^* of the unfiltered one-dimensional spectrum is then $0{\cdot}034k_d$ and $0{\cdot}029k_d$ for runs 1 and 2 respectively, whereas k^* is $0{\cdot}068k_d$ and $0{\cdot}057k_d$.

Several facts are evident from the above results. First, $k^\dagger$, a parameter of model 4, is not k^*; $k^\dagger/k^* \simeq 1{\cdot}32$. Second, the transitional wavenumbers in the filtered spectra, $(k_1^*)_{\mathrm{meas}} = 0{\cdot}04k_d$ and $0{\cdot}03k_d$, are different from the values of k_1^* from the unfiltered spectra, $k_1^* = 0{\cdot}034k_d$ and $0{\cdot}029k_d$; the percentage discrepancy between the transitional wavenumber in the data ($0{\cdot}04k_d$ and $0{\cdot}03k_d$) is greater than the percentage

Data set	ν/D	k^*/k_d	q
Grant *et al.* (1968)	9·2	0·041 ± 0·013	6·2 ± 1·4
Champagne *et al.* (1977) and Williams & Paulson (1977)	0·72	0·054 ± 0·001	5·1 ± 0·06
Gibson *et al.* (1970*a*)	700	0·062 ± 0·006	4·7 ± 0·2

TABLE 2. Values of k^*/k_d and q determined by comparing model 4 with experiments.

discrepancy between the k_1^* values ($0{\cdot}034k_d$ and $0{\cdot}029k_d$) that result from the model fit to the data. Thus the filtering increases the value of the transitional wavenumber by an amount that depends on the value of the cut-off wavenumber relative to k^*. Third, the transitional wavenumbers k^* and k_1^* are unequal; for large ν/D we have $k^*/k_1^* \simeq 1{\cdot}98$. Fourth, in order to interpret low-pass filtered data, such as those of Gibson *et al.* (1970*a*), in terms of the universal constant k^*/k_d the use of a model of the scalar spectrum is needed.

The values of k^*/k_d determined by comparing model 4 with the experiments performed by Grant *et al.* (1968), the two runs by Gibson *et al.* (1970*a*), and by Champagne *et al.* (1977) and Williams & Paulson (1977) are brought together in table 2. These values of k^*/k_d are all consistent within experimental uncertainties. This lends strong support to the assertion that the bump observed in the temperature spectrum in air ($\nu/D = 0{\cdot}72$) is the beginning of a viscous–convective range. From top to bottom in table 2 the experiments are listed from highest Reynolds number to lowest; while the k^*/k_d values increase from top to bottom. This suggests, but does not prove, that k^*/k_d might decrease with increasing Reynolds number.

Model 4 can be used to determine Batchelor's constant q, which is defined by $\gamma = -q^{-1}(\epsilon/\nu)^{\frac{1}{2}}$. For the viscous–convective range, comparison of (6) and (15) gives $\gamma = -\frac{1}{5}\Lambda$. Then (20), with k^3 replaced by $k^\dagger$, gives

$$q = \tfrac{11}{9}\beta(k^\dagger/k_d)^{-\frac{2}{3}} = 1{\cdot}016\beta(k^*/k_d)^{-\frac{2}{3}}. \tag{21}$$

Equation (21) is very nearly the same as is obtained by equating (4) and (6) at $k = k^*$. Batchelor's constant, as determined from the k^*/k_d values, is also given in table 2; β is assumed to be 0·72 for this purpose. The values of q in table 2 tend to increase with increasing Reynolds number.

5.4. *Comparison with temperature fluctuations in mercury*

Clay (1973) has measured temperature fluctuations in mercury ($Pr \simeq 0{\cdot}018$) in order to observe an inertial–diffusive range. Two power laws were observed over very limited ranges of wavenumber. A k^{-3} power law was found for $0{\cdot}025 < k/k_d < 0{\cdot}039$. At the highest observable wavenumbers the spectrum steepened to a $k^{-\frac{17}{3}}$ power law between $k/k_d = 0{\cdot}12$ and 0·23. The observed values of β_1 increase with increasing Reynolds number from roughly 0·3 to 0·75. The β_1 values did not level off with increasing Reynolds number even though an inertial–convective range was observable at the highest Reynolds numbers attained.

Both the three-dimensional and the one-dimensional spectra are computed for $Pr = 0{\cdot}018$ using model 4 with the parameters obtained from the comparison with the data of Champagne *et al* (1977). The dissipation spectra are presented in figure 9 along

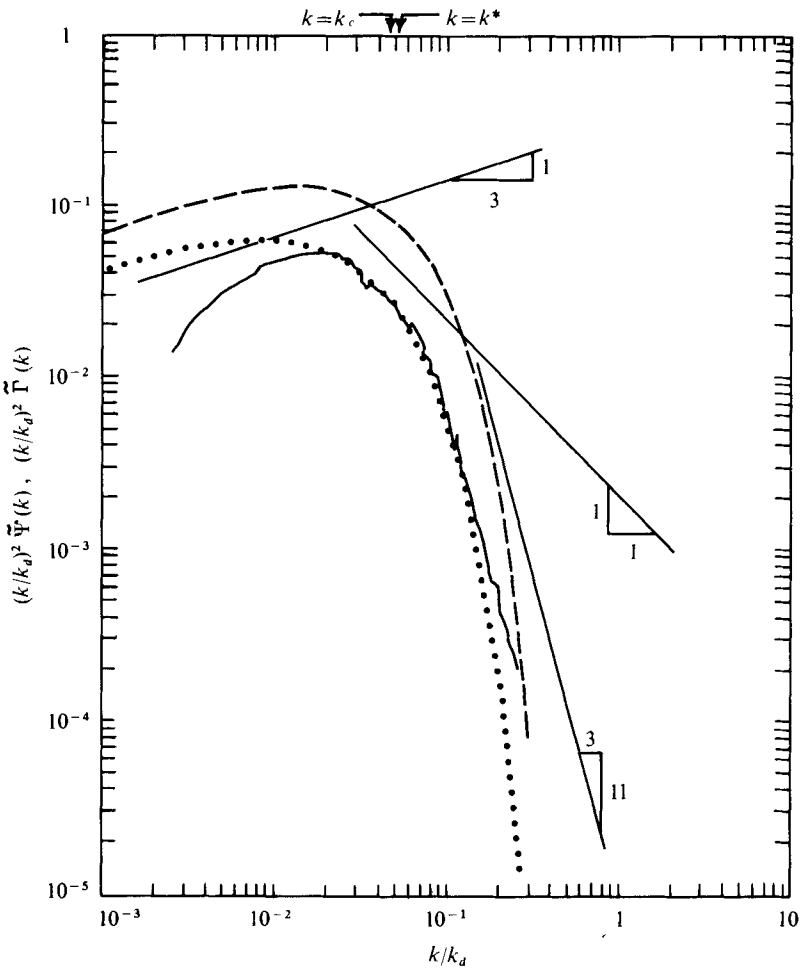

FIGURE 9. Comparison of model 4 with the temperature spectrum in mercury measured by Clay (1973). The dashed and dotted curves are the model three-dimensional and one-dimensional spectra, respectively. The solid curve is the measured one-dimensional spectrum.

with the measured temperature spectrum in mercury that appears in figure 19 of Clay (1973). The straight lines having slopes $\frac{1}{3}$, -1, and $-\frac{11}{3}$ correspond to spectral power laws $k^{-\frac{5}{3}}$, k^{-3}, and $k^{-\frac{17}{3}}$, respectively. The model spectrum was determined using $\beta_1 = 0{\cdot}43$. The scaling in figure 19 of Clay (1973) is apparently in error; the spectral values must be multiplied by 0·54 in order that the area under the scaled dissipation spectrum equals $\frac{1}{6}Pr$ as it should. In view of this scaling error and the variation of the measured values of β_1 with Reynolds number, the measured spectrum in figure 9 was displaced vertically to obtain a best fit to the model. Because of this displacement, it cannot be said that the model compares favourably with the data. However, it is seen that the shape of the model spectrum follows that of Clay's data for wavenumbers between $k/k_d = 0{\cdot}02$ and 0·2. Of course, none of the models developed here have a power-law inertial–diffusive range. In addition, the model spectrum was used to estimate the effect of the fluctuating-convection-velocity aliasing for Clay's experiment; this effect was found to be negligible.

The inertial–convective range power law of the model appears for k/k_d smaller than about 0·003. Such low wavenumbers lie within the variance-containing range of the data. Thus the model interprets the data as having no true inertial–convective range because the Péclet number is too small.

In previous sections it was found that $k^*/k_d \simeq 0{\cdot}05$. Therefore, for $Pr \ll 1$ the model predicts that there is a transition from an inertial–diffusive range to a viscous–diffusive range at wavenumbers near $k^* \simeq 0{\cdot}05k_d$. This suggests the conjecture that the steepening of the measured spectrum from k^{-3} to $k^{-\frac{17}{5}}$ near $k = 0{\cdot}05k_d$ is due to a transition from an inertial–diffusive range to a viscous–diffusive range. Since the transitional wavenumber k^* is rather small, e.g. $k^*/k_d \simeq 0{\cdot}05$, it is evident that the inertial–diffusive range for $Pr = 0{\cdot}018$ might be of very limited extent. A convincing measurement of an inertial–diffusive range would require $\nu/D \simeq 10^{-3}$ and a high Reynolds number flow.

6. Conclusion

Four models of the scalar spectral transfer function are developed and the resulting scalar spectra are compared with experiment. These models are applicable for arbitrary ν/D for high Reynolds number flow and all have the expected $k^{-\frac{5}{3}}$ variation in the inertial–convective range and the k^{-1} variation in the viscous–convective range. Models 1 and 3 give a good fit to the dissipation spectra found by Champagne *et al.* (1977) and Williams & Paulson (1977); however, these models do not represent the data well in the inertial–convective range. Models 2 and 4 are in good agreement with the data gathered by Champagne *et al.* and by Williams & Paulson. An outstanding feature of the temperature spectra observed by these experimenters is the 'bump' at high wavenumbers. The models show that this bump is a tendency to a viscous–convective range at wavenumbers lower than the wavenumbers at which diffusion rapidly decreases the temperature spectrum.

Values of the transitional wavenumber k^* are determined from measurements and are given in table 2. These values appear to increase slightly with decreasing Reynolds number; whether or not this effect is real remains a matter for further experimentation and theoretical insight. Using the values of k^*/k_d from the large ν/D experiments of Grant *et al.* (1968) and Gibson *et al.* (1970*a*), the models then predict a bump in the temperature spectrum in air, $Pr = 0{\cdot}72$. Thus a consistent picture emerges for the spectrum of scalar fluctuations for arbitrary ν/D.

For constant k^*/k_d, the ratio of k^* to the transitional wavenumber observed in a one-dimensional scalar spectrum is a function of ν/D and also of the location of a low-pass filter cut-off, if any. The transitional wavenumber k_1^* is defined in (17) only for asymptotically large ν/D; model 4 gives $k^*/k_1^* = 1{\cdot}98$.

The values found for k^*/k_d, namely about 0·05, have the following implications. First, values of β_1 determined from the level of the temperature spectrum in air measured in moderate Reynolds number flows may be too large owing to the presence of the bump. An accurate determination of β_1 requires the observation of an inertial–convective range in the temperature spectrum in air at wavenumbers less than about $0{\cdot}03k_d$. Second, the inertial–diffusive range for temperature fluctuations in mercury is of very limited extent; a convincing observation of the inertial–diffusive range would require $\nu/D \simeq 10^{-3}$ and a high Reynolds number flow.

Model 4 gives the best fit to the data obtained by Champagne *et al.* (1977) and by Williams & Paulson (1977). This model can then predict the shape of such spectra as the humidity spectrum, which has not been measured at high wavenumbers because of limited frequency response of the sensors. The predicted humidity spectrum and temperature–humidity co-spectrum given by Hill (1978) have a bump corresponding to that observed in temperature spectra in air. Model 4 is recommended for use in computing quantities relevant to optical and radio wave propagation in turbulent media. Such an application to optical propagation is made by Hill & Clifford (1978). An application to VHF radio wave scattering from turbulence-induced fluctuations in the D region ionization is made by Hill (1976).

The author thanks S. A. Bowhill, P. K. Rastogi, J. C. Wyngaard, C. A. Friehe, C. H. Gibson and J. P. Clay for their helpful discussions, and F. H. Champagne, C. A. Friehe, J. C. LaRue, R. M. Williams, C. A. Paulson, and J. P. Clay for allowing the use of their data. The author is indebted to R. M. Jones for his help with the computations. Figure 8 is taken, in part, from page 435 of the paper by Grant *et al.* (1968) and is reproduced here by permission of the Cambridge University Press. The research described was supported by NSF grant ATM-73-06485 and by the National Research Council through the Resident Research Accociateship program.

REFERENCES

Batchelor, G. K. 1959 Small-scale variation of convected quantities like temperature in turbulent fluid. Part 1. General discussion and the case of small conductivity. *J. Fluid Mech.* **5**, 113–133.

Batchelor, G. K., Howells, I. D. & Townsend, A. A. 1959 Small-scale variation of convected quantities like temperature in turbulent fluid. Part 2. The case of large conductivity. *J. Fluid Mech.* **5**, 134–139.

Boston, N. E. & Burling, R. W. 1972 An investigation of high wavenumber temperature and velocity spectra in air. *J. Fluid Mech.* **55**, 473–492.

Bugnolo, D. S. 1972 Turbulence in weakly ionized plasma. *J. Plasma Phys.* **8**, 143–158.

Champagne, F. H., Friehe, C. A., LaRue, J. C. & Wyngaard, J. C. 1977 Flux measurements, flux-estimation techniques, and fine-scale turbulence measurements in the unstable surface layer over land. *J. Atmos. Sci.* **34**, 515–530.

Clay, J. P. 1973 Turbulent mixing of temperature in water, air and mercury. Ph.D. thesis, University of California at San Diego.

Corrsin, S. 1951 On the spectrum of isotropic temperature fluctuations in isotropic turbulence. *J. Appl. Phys.* **22**, 469–473.

Corrsin, S. 1961 The reactant concentration spectrum in turbulent mixing with a first-order reaction. *J. Fluid Mech.* **11**, 407–416.

Corrsin, S. 1964 Further generalization of Onsager's cascade model for turbulent spectra. *Phys. Fluids* **7**, 1156–1159.

Garosi, G. A., Bekefi, G. & Schulz, M. 1970 Response of a weakly ionized plasma to turbulent gas flow. *Phys. Fluids* **13**, 2795–2809.

Gibson, C. H. 1968 Fine structure of scalar fields mixed by turbulence. II. Spectral theory. *Phys. Fluids* **11**, 2316–2327.

Gibson, C. H., Lyon, R. R. & Hirschsohn, I. 1970*a* Reaction product fluctuations in a sphere wake. *A.I.A.A. J.* **8**, 1859–1863.

Gibson, C. H. & Schwarz, W. H. 1963 The universal equilibrium spectra of turbulent velocity and scalar fields. *J. Fluid Mech.* **16**, 365–386.

GIBSON, C. H., STEGEN, G. R. & WILLIAMS, R. B. 1970*b* Statistics of the fine structure of turbulent velocity and temperature fields measured at high Reynolds number. *J. Fluid Mech.* **41**, 153–167.

GRANATSTEIN, V. L., LEVINE, A. M. & SUBRAMANIAN, M. 1971 Laser probing of a weakly ionized turbulent gas: comparison of neutral and plasma fluctuations. *Phys. Fluids* **14**, 2581–2587.

GRANT, H. L., HUGHES, B. A., VOGEL, W. M. & MOILLIET, A. 1968 The spectrum of temperature fluctuations in turbulent flow. *J. Fluid Mech.* **34**, 423–492.

HILL, R. J. 1976 Small-scale fluctuations in D-region ionization due to hydrodynamic turbulence. *Aeron. Rep.* 75, Dep. Elec. Eng., University of Illinois, Urbana, IL 61801.

HILL, R. J. 1978 Spectra of fluctuations in refractivity, temperature, humidity, and the temperature-humidity cospectrum in the inertial and dissipation ranges. *Radio Science* (to be published).

HILL, R. J. & CLIFFORD, S. F. 1978 The modified spectrum of atmospheric temperature fluctuations and its application to optical propagation. *J. Opt. Soc. Am.* (to be published).

KRAICHNAN, R. H. 1968 Small-scale structure of a scalar field convected by turbulence. *Phys. Fluids* **11**, 945–953.

KUYEL, B. & GRUBER, S. 1973 Experimental turbulence spectra in neutral and ion components of a weakly ionized gas. *Phys. Fluids* **16**, 1842–1847.

LEE, T. D. 1952 On some statistical properties of hydrodynamical and magneto-hydrodynamical fields. *Quart. Appl. Math.* **10**, 69–74.

LEITH, C. E. 1968 Diffusion approximation for turbulent scalar fields. *Phys. Fluids* **11**, 1612–1617.

LIN, S. C. & LIN, S. C. 1973 Study of strong temperature mixing in subsonic grid turbulence. *Phys. Fluids* **16**, 1587–1598.

LIN, J. T. 1972 Velocity spectrum of locally isotropic turbulence in the inertial and dissipation ranges. *Phys. Fluids* **15**, 205–207.

MCCONNELL, S. 1976 The fine structure of velocity and temperature measured in the laboratory and atmospheric marine boundary layer. Ph.D. thesis, University of California, San Diego.

MCKELVEY, K. N., YIEH, H. N., ZAKANYCZ, S. & BRODKEY, R. S. 1975 Turbulent motion, mixing, and kinetics in a chemical reactor configuration. *A.I.Ch.E. J.* **21**, 1165–1176.

MJOLSNESS, R. C. 1975 Diffusion of a passive scalar at large Prandtl number according to the abridged Lagrangian interaction theory. *Phys. Fluids* **18**, 1393–1394.

NYE, J. O. & BRODKEY, R. S. 1967 The scalar spectrum in the viscous-convective subrange. *J. Fluid Mech.* **29**, 151–163.

OBOUKHOV, A. M. 1949 Structure of the temperature field in turbulent flow. *Izv. Akad. Nauk SSSR, Ser. Geogr. i Geofiz.* **13**, 58–69.

ONSAGER, L. 1949 Statistical hydrodynamics. *Nuovo Cimento*, Suppl. 6, pp. 279–287.

PAO, Y. H. 1964 Statistical behavior of a turbulent multicomponent mixture with first-order reactions. *A.I.A.A. J.* **2**, 1550–1559.

PAO, Y. H. 1965 Structure of turbulent velocity and scalar fields at large wavenumbers. *Phys. Fluids* **8**, 1063–1075.

PAQUIN, J. E. & POND, S. 1971 The determination of the Kolmogoroff constants for velocity, temperature and humidity fluctuations from second- and third-order structure functions. *J. Fluid Mech.* **50**, 257–269.

POND, S., SMITH, S. D., HAMBLIN, P. F. & BURLING, R. W. 1966 Spectra of velocity and temperature fluctuations in the atmospheric boundary layer over the sea. *J. Atmos. Sci.* **23**, 376–386.

RUST, J. H. & SESONSKE, A. 1966 Turbulent temperature fluctuations in mercury and ethylene glycol in pipe flow. *Int. J. Heat Mass Transfer* **9**, 215–227.

SCHMITT, K. F., FRIEHE, C. A. & GIBSON, C. H. 1978 Humidity sensitivity of atmospheric temperature sensors by salt contamination. *J. Phys. Ocean.* **8**, 151–161.

WILLIAMS, R. M. & PAULSON, C. A. 1977 Microscale temperature and velocity spectra in the atmospheric boundary layer. *J. Fluid Mech.* **83**, 547–567.

WYNGAARD, J. C. & CLIFFORD, S. F. 1977 Taylor's hypothesis and high-frequency turbulence spectra. *J. Atmos. Sci.* **34**, 922–929.